Shear thinning in concentrated dispersions



1996 J. Phys.: Condens. Matter 8 8145

(http://iopscience.iop.org/0953-8984/8/43/011)

J. Phys.: Condens. Matter **8** (1996) 8145–8156. Printed in the UK

# Shear thinning in concentrated dispersions

T S Chow

Xerox Corporation, Wilson Center for Research and Technology, 800 Phillips Road, 0114-39D, Webster, NY 14580, USA

Received 16 April 1996, in final form 30 July 1996

**Abstract.** A theory is presented to predict the effective shear viscosity of concentrated dispersions in steady state shear flow as a function of the volume fraction, particle size, interparticle interactions, and shear rate. Shear thinning has been qualitatively argued to be a result of shear-induced change in microstructure, which we shall discuss in terms of the distribution function. Analysing the distribution function and the microscopic stress tensor, we have derived a memory function in steady state shear flow. It is used to calculate all the key features of shear thinning quantitatively without any adjusting parameter. The predicted shear-rate-dependent effective shear viscosity is in good agreement with the experiments of sterically stabilized colloidal suspensions. Since shear thinning has been observed in steady state shear flow as well as in oscillatory shear flow, the difference between these two flows will also be discussed in terms of the distribution functions and structural relaxations.

## 1. Introduction

Colloidal dispersions have interesting and complex flow behaviour because the macroscopic stresses are sensitive to the nonequilibrium microstructure, which in turn depends on the composition, flow field, and particle interactions. Experimental data [1–5] for shear viscosity exhibit two key features: they diverge strongly as the particle volume fraction ($\phi$) of colloidal particles is increased and they exhibit strong shear rate dependence, decreasing with increased shear rate. The shear viscosity is Newtonian for dilute suspensions, and becomes non-Newtonian (shear rate dependent) for semidilute suspensions [3, 6–8]. Shear thinning becomes more pronounced as $\phi$ approaches a percolation threshold $\phi_c$. This unusual phenomenon has been observed for colloidal dispersions, but not for polymer solutions. These effects have been qualitatively argued (see [2] where additional references can also be found) to be the result of shear-induced microstructure within the suspension; however, there is no quantitative theoretical analysis available at the present time. It is the purpose of this paper to develop one.

Polymeric liquids [9–11] also exhibit non-Newtonian flow behaviour, but they recover from finite stresses and do not show the above-mentioned shear thinning as $\phi \to \phi_c$. This reflects the fundamentally different microstructures in colloidal suspensions and polymeric liquids. In contrast to the long-range interactions in macromolecular systems, short-range interparticle forces govern the microstructure in colloidal dispersions and the magnitude decreases with increasing separation. In spite of these differences, the microscopic theory of polymeric liquids [9, 10] should serve as a useful basis in the present study. Shear thinning is generally believed to result from shear-induced change in microstructure. On the basis of the approach given in [9] and [10], the microstructure is characterized in terms

0953-8984/96/438145+12$19.50  

of the distribution function ($\psi$) in section 2. An effective-medium approximation for $\psi$ will then be used to solve our problem. Instead of using the usual Kirkwood formula [12] for the stress tensor for polymer solutions, we find that it is more convenient in the case of disperse systems to use the method of statistical mechanics to analyse the stress tensor in the derivation of the effective shear viscosity in section 3. The main result of the shear-rate-dependent shear viscosity in steady state shear flow is derived in section 4. In the final discussion of section 5, the salient features of non-Newtonian behaviour in the vicinity of $\phi_c$ are calculated. The basic differences between the nonlinear viscosity in steady state shear flow and the linear dynamic viscosity in oscillatory shear flow are discussed.

## 2. Colloidal dynamics

The dynamics of disperse systems can be described by the time-dependent distribution function $\psi(\boldsymbol{R}_1, \boldsymbol{R}_2, \ldots, \boldsymbol{R}_N, t)$ where $\boldsymbol{R}_i$ is the position of the $i$th colloidal particle and $t$ is time. The probability ($\psi$) of finding a particle at a given point and time is governed by the equation of continuity [9]

$$\frac{\partial \psi}{\partial t} = -\sum_{i=1}^{N} \left( \frac{\partial}{\partial \boldsymbol{R}_i} \cdot \dot{\boldsymbol{R}}_i \psi \right) \tag{1}$$

where $\dot{\boldsymbol{R}}_i$ is the velocity of the $i$th particle. This equation simply states that when a particle leaves one location it has to turn up in another. Equation (1) needs an expression for the velocity $\dot{\boldsymbol{R}}_i$, which can be obtained by analysing the equation of motion of individual particles. Let us begin with dilute suspensions: the colloidal particle can move freely through the surrounding solent molecules. Both hydrodynamic and non-hydrodynamic forces are acting on the particle. The equations of motion can be written down as

$$m_i \ddot{\boldsymbol{R}}_i = -\zeta_0(\dot{\boldsymbol{R}}_i - \boldsymbol{v}_i) + \boldsymbol{F}_i \qquad i = 1, 2, \ldots, N \tag{2}$$

where $\ddot{\boldsymbol{R}}_i$ is the acceleration of the $i$th particle and $m_i$ is the mass. The first term on the right-hand side is the hydrodynamic drag, $\zeta_0 = 6\pi\eta_2 a$ is the frictional coefficient, $\eta_2$ is the solvent viscosity, and $a$ is the particle radius. $\boldsymbol{v}_i$ is the flow velocity which would have existed at the point of location of the $i$th particle if this particle had been absent. The total non-hydrodynamic force is [13]

$$F_i = -(\partial/\partial \boldsymbol{R}_i)(kT \ln \psi + U) \tag{3}$$

where $k$ is the Boltzmann constant and $T$ is the temperature. The first term is the Brownian force, and the second is the interparticle force with its potential energy $U$. The acceleration term on the left-hand side of equation (2) is assumed to be negligible. That is

$$\dot{\boldsymbol{R}}_i = (1/\zeta_0)\boldsymbol{F}_i + \boldsymbol{v}_i. \tag{4}$$

For concentrated dispersions, (4) can be generalized to

$$\dot{\boldsymbol{R}}_i = \sum_{j=1}^{N} \boldsymbol{H}_{ij} \boldsymbol{F}_j + \boldsymbol{v}_i \tag{5}$$

where $\boldsymbol{H}_{ij}$ is the mobility tensor. As mentioned in (2), $\boldsymbol{v}_i$ in (4) and (5) is due to the imposed flow field, which is negligible in linear oscillatory shear flow [8] but will be important in the present study of nonlinear steady state shear flow. More specific analysis and discussion will be given in sections 4 and 5. (5) accounts for the many-body interactions between particles and solvent molecules in a formal way. Of course, it *cannot* be solved as it stands

and approximations have to be made later in order to proceed. Combining (1) and (5), we obtain

$$\frac{\partial \psi}{\partial t} = \sum_{i=1}^{N} \frac{\partial}{\partial \boldsymbol{R}_i} \cdot \left[ \sum_{j=1}^{N} \boldsymbol{H}_{ij} \left( kT \frac{\partial \psi}{\partial \boldsymbol{R}_j} + \psi \frac{\partial U}{\partial \boldsymbol{R}_j} \right) - \boldsymbol{v}_i \psi \right] \tag{6}$$

which is termed the Smoluchowski equation for disperse systems. It may also be called the Fokker–Planck equation. Formally, equation (6) looks quite similar to that for polymeric liquids [10].

In practice (5) and (6) will be solved by using an effective one-particle approximation in a self-consistent manner. Physically, it consists of a colloidal particle moving through the surrounding medium whose viscosity is equal to the *effective* shear viscosity ($\eta$) of the dispersion. $\eta$ has yet to be determined. This allows for a nonlinear response to the interactive system. In the self-consistent model, the mobility tensor is written as

$$\boldsymbol{H}_{ij} = [\boldsymbol{I}/\zeta(\phi)]\delta_{ij} \tag{7}$$

where $\boldsymbol{I}$ is the unit tensor, and $\zeta(\phi) = 6\pi a \eta(\phi)$. For dilute solutions in *shear* ($\zeta(\phi) = \zeta_0$), (7) has the exact form used in Rouse's model (see (4.3) in [10]) and in Debye's free draining model. Since the general philosophy of Hartree–Fock [14] was introduced, the use of the one-particle self-consistent approximation to solve a many-body problem has been published frequently in various forms for different subjects with great success. This approximation has also been mentioned in the literature as an effective-medium theory. The 'particle' can be thought of as an electron, molecule, Brownian particle, or filler in composites in the study of the electrical [14], optical [15], mechanical [16], and rheological [17] properties of complex materials. In the present case of colloidal dispersions, the one-particle approximation has already been utilized in analysing the shear viscosity [17]. Shear thinning is the topic of this paper. The one-particle approximation with effective viscosity will be solved self-consistently with (12), (20), (21), (22), (24), and (25) to be derived and discussed in the rest of the paper. The effect of microstructure due to the many-body interactions mentioned in (5) and the interparticle force in (3) are taken into account collectively in terms of the effective viscosity. Using (7), we obtain

$$\frac{\partial \psi}{\partial t} = \frac{\partial}{\partial \boldsymbol{R}} \cdot \left[ D \frac{\partial \psi}{\partial \boldsymbol{R}} - (\boldsymbol{v}\psi) \right] \tag{8}$$

where $D = kT/\zeta$ is the effective diffusion coefficient. Both $D$ and $\zeta$ are functions of $\eta$. What we have in (8) is the reduced distribution function of a Brownian particle which is related to (1) formally by

$$\psi^{(1)}(\boldsymbol{R}_1, t) = \int \psi(\boldsymbol{R}_1, \boldsymbol{R}_2, \ldots, \boldsymbol{R}_N, t)\, \mathrm{d}\boldsymbol{R}_2\, \mathrm{d}\boldsymbol{R}_3, \ldots, \mathrm{d}\boldsymbol{R}_N.$$

For simplicity, we have dropped the superscript of $\psi^{(1)}$ and subscript of $\boldsymbol{R}_1$ on the left-hand side of the above equation as the symbol shown in (8). The further discussion of the reduced distribution function can be found in a standard text of statistical mechanics, and the specific discussion of Brownian particles in [18].

The shear-induced change in microstructure is described by the particle distribution function $\psi$ in (8) under the influence of a macroscopic velocity field. Using $\psi$, we shall analyse the effective viscosity $\eta$ as a function of $\eta_2$, $a$, $\phi$, $U$, and shear rate $\gamma$ in the rest of the paper.

## 3. Effective shear viscosity

In the development of microscopic theory of the non-Newtonian viscosity [9, 10], the principal aim is the evaluation of the stress tensor. By using the method of statistical mechanics, the *configuration average* of the local stress tensor $\sigma_{\alpha\beta}$ created by a given flow field $\boldsymbol{v}(\boldsymbol{r})$ and Brownian motion in the system is determined by

$$\overline{\sigma_{\alpha\beta}(\boldsymbol{r})} = \int \sigma_{\alpha\beta}(\boldsymbol{r}, \boldsymbol{R})\psi(\boldsymbol{R})\,\mathrm{d}\boldsymbol{R}. \tag{9}$$

The *spatially dependent* stress tensor on the left-hand side of (9) is equal to the configuration average of particles with the stress tensor and the distribution function on the right. (9) has the general form of the statistical average of a physical quantity, which can be a scalar, vector, or tensor. The exact form of (9) can be found in [10] (see equation (3.117) on p 71).

*Spatial averaging* $\overline{\sigma_{\alpha\beta}(r)}$ over the total volume $V$ containing $N$ colloidal particles gives the *spatially independent* stress components:

$$\langle\sigma_{\alpha\beta}\rangle = \frac{1}{V}\int_v \overline{\sigma_{\alpha\beta}(\boldsymbol{r})}\,\mathrm{d}\boldsymbol{r} = \frac{1}{V}\left[\int_{v_2} \overline{\sigma_{\alpha\beta}(\boldsymbol{r})}\,\mathrm{d}\boldsymbol{r} + \sum_{i=1}^{N}\int_{v_1} \overline{\sigma_{\alpha\beta}(\boldsymbol{r})}\,\mathrm{d}\boldsymbol{r}\right] \tag{10}$$

where $V$ is the total volume and $V_1$ and $V_2$ are the volumes of the particles and solvent, respectively. In general, the second-order stress tensor is related to the second-order strain rate tensor by a fourth-order viscosity tensor [17]. Since we are only interested in the shear flow in this paper, the effective shear viscosities of disperse systems can then be obtained from

$$\eta_{\alpha\beta} \equiv \langle\sigma_{\alpha\beta}\rangle/2\langle e_{\alpha\beta}\rangle = \langle\sigma_{\alpha\beta}\rangle/2e^0_{\alpha\beta} \qquad \alpha \neq \beta \tag{11}$$

where $e^0_{\alpha\beta}$ is a constant strain rate applied to the system. Substituting (11) into (10) and noting that the dispersed system as a whole has to be macroscopically homogeneous, i.e.,

$$\frac{1}{V}\int_v \overline{e_{\alpha\beta}(\boldsymbol{r})}\,\mathrm{d}\boldsymbol{r} = e^0_{\alpha\beta}$$

we obtain the effective shear viscosity of hard-sphere dispersions

$$\eta = \eta_2(1-\phi) + \frac{\phi\langle\sigma_{\alpha\beta}\rangle_1}{2e^0_{\alpha\beta}} \qquad \alpha \neq \beta \tag{12}$$

where the hard-sphere fluid is isotropic (i.e. $\eta = \eta_{\alpha\beta}$), $\phi = \sum$ (volume of particles, $V_1) = NV_1/V$ is the volume fraction, and

$$\langle\sigma_{\alpha\beta}\rangle_1 = \frac{1}{V_1}\int_{v_1} \overline{\sigma_{\alpha\beta}(\boldsymbol{r})}\,\mathrm{d}\boldsymbol{r}. \tag{13}$$

(8), (9), and (12) together may be regarded as a constitutive equation for a given velocity field. The distribution function is obtained from (8) and the nonlinear viscosity from (12).

## 4. Steady state shear flow

Probably the single most important characteristic of concentrated dispersions is the fact that they have a shear-rate-dependent viscosity. Choose the centre of a spherical particle as the origin of spatial coordinates, and consider the steady shear flow:

$$\boldsymbol{v} = \gamma z\boldsymbol{j} \tag{14}$$

where $\gamma = 2e^0_{yz}$ is the shear rate. The inverse of the shear rate $(1/\gamma)$ is a time scale characterizing the shear thinning and structural relaxation of colloidal dispersions. Substituting (14) into (8), using (9), and noting $\psi$ vanishes at infinity, we find by partial integrations

$$D\frac{\mathrm{d}^2\overline{\sigma_{yz}}}{\mathrm{d}y^2} + \gamma z\frac{\mathrm{d}\overline{\sigma_{yz}}}{\mathrm{d}y} = 0. \tag{15}$$

The solution of (15) is

$$\overline{\sigma_{yz}(\boldsymbol{r})} = A + B\exp\left(-\frac{\gamma\zeta yz}{kT}\right) \tag{16}$$

where $A$ and $B$ are constants. Substituting (16) into (13) gives

$$\langle\sigma_{yz}\rangle_1 = A + \frac{B}{V_1}\int_{v_1}\left(1 - \frac{\gamma\zeta yz}{kT} + \cdots\right)\mathrm{d}\boldsymbol{r}. \tag{17}$$

Introducing the polar angles $\theta$ and $\varphi$,

$$y = r\sin\theta\sin\varphi \qquad z = r\cos\theta \tag{18}$$

and noting $\gamma\zeta yz$ is the energy induced by the flow field, one obtains

$$\langle yz\rangle_1 = \frac{3}{\pi a^3}\int_0^{\pi}\int_0^{\pi/2}\int_0^{a}(r^2\sin\theta\sin\varphi\cos\theta)r^2\sin\theta\,\mathrm{d}r\,\mathrm{d}\theta\,\mathrm{d}\varphi = \frac{2a^2}{5\pi}. \tag{19}$$

The shear thinning phenomenon has been observed in steady state shear flow as well as in oscillatory shear flow. Therefore, it is important to see the essential difference in the structural relaxation of these two flows to be discussed in section 5. In order to make direct comparison later, the shear-rate-dependent effective shear viscosity $(\eta)$ derived from (12) and (16)–(19) is recast in the form of (26) for oscillatory shear flow:

$$\eta(\gamma,\phi) = \eta_\infty(\phi) + [\eta_0(\phi) - \eta_\infty(\phi)]Q[\eta(\gamma,\phi)] \tag{20}$$

and

$$Q[\eta(\gamma,\phi)] = \exp\left[-2.4\phi\frac{a^3\gamma}{kT}\eta(\gamma,\phi)\right] \tag{21}$$

where $\eta_0$ and $\eta_\infty$ are the limits of viscosity at low and high shear rates. Both $\eta_0$ and $\eta_\infty$ are *independent of time and space*. We have shown [8] that $Q$ is the memory function which goes to unity as $\eta \to \eta_0$, and to zero as $\eta \to \eta_\infty$. The definition of $Q$ as a memory function in the form of (20) is very general and applies to all materials exhibiting structural relaxations [19]. There is *no adjusting parameter* in $Q$ which includes the effects of Brownian motion and shear-rate-dependent structural relaxation. The two constants $A$ and $B$ in (16) are related to the limits of viscosity $\eta_0$ and $\eta_\infty$ in (20) by

$$\eta_\infty(\phi) = [A\phi + B(1-\phi)]/\gamma$$

and

$$\eta_0(\phi) - \eta_\infty(\phi) = B/\gamma.$$

In addition to the shear rate, both $\eta$ and $Q$ are functions of particle size, concentration, and limits of viscosity. (20) and (21) have to be solved numerically. Figure 1 shows the comparison between the calculated results and experimental data [1, 4] for 50% monodispersions of polystyrene spheres of various sizes in different media such as water, benzyl alcohol, or *meta*-cresol. The diameter of the hard spheres varies from 46 to 180 nm.

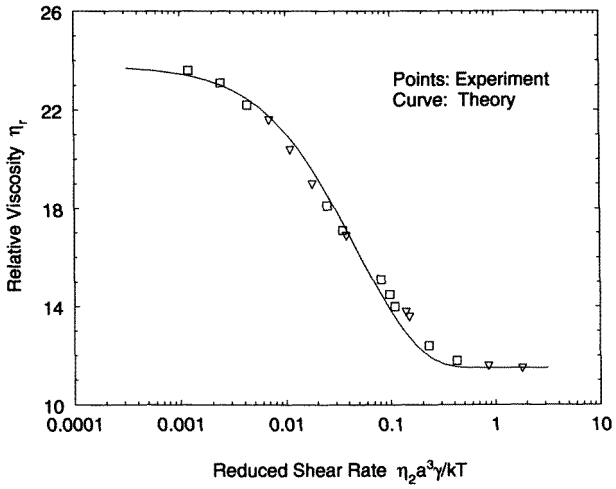


**Figure 1.** The calculated relative shear viscosity versus reduced shear rate (from (20) and (21)) is compared with the experimental data [1, 4] for polystyrene spheres of various sizes dispersed in water, benzyl alcohol, and *meta*-cresol. The volume fraction is $\phi = 0.5$.

## 5. Results and discussion

Hard-sphere repulsion provides a convenient basis for analysing the rheological behaviour of stable dispersions. When contributions from the hydrodynamic and intermolecular interactions are included in the analysis of stable hard-sphere dispersions, the shear viscosities at the low- and high-shear-rate limits are derived.

The hydrodynamic effect is the dominant effect on the relative shear viscosity at the high-shear-rate limit [17, 20]:

$$\eta_r(\infty, \phi) \equiv \eta_\infty(\phi)/\eta_2 = \exp(2.5\phi/(1-\phi)). \tag{22}$$

The difference in the limiting viscosities at the low and high shear rates is a result of the energy being dissipated through the loss in kinetic energy, which can be related directly to the interparticle potential by [21]

$$\Delta\eta_r(\phi) = -\iint \rho(r_{12}) r_{12} \frac{\partial V(r_{12})}{\partial r_{12}} \,\mathrm{d}\boldsymbol{r}_1 \,\mathrm{d}\boldsymbol{r}_2 \tag{23}$$

where $V$ is the nondimensional pair potential, $r_{12} = |\boldsymbol{r}_1 - \boldsymbol{r}_2|$ is the distance between the centres of two spheres, and $\rho$ is the pair distribution function. For dilute suspensions, we consider the interparticle potential $(U)$ has the form [8] $U(r) = -u$ for $r < 2a$ and zero for $r \geqslant 2a$, where $u$ is called the repulsive interparticle potential. The equilibrium radial distribution function is $g_0 = V = \exp(-U/kT)$. For incompressible fluids, we approximate $\rho \sim g_0\psi$ with $\psi$ being determined by the Kirkwood–Smoluchowski equation [22] which is a special case of (6) and (8). This leads to $\Delta\eta_r$ of dilute suspensions. A detailed analysis and in-depth discussion of $U$, $g_0$, $\psi$, and $\Delta\eta_r$ can be found in [8]. The 'hard' sphere considered here has very high but *not infinite* rigidity, which is always true in a real system. Therefore, the pair potential is finite.

As the volume fraction of colloidal particles increases, the many-body interactions between the particles and the equilibrium microstructure have been included in the analysis.

The interactions of the particle as it propagates through a dense dispersion has been evaluated by using the Feynman diagram. When the detailed analysis is carried out, an expression for the zero-shear viscosity is derived [8]:

$$\eta_r(0,\phi) \equiv \eta_0(\phi)/\eta_2 = \eta_r(\infty,\phi) + (\phi/\phi_c)^2/[1-(\phi/\phi_c)^2]P. \tag{24}$$

Here the probability $P$ is produced by the interactions of the colloidal particles with each other and solvent molecules. It is equal to the maximum packing fraction of a unit structural volume filled with spheres. The percolation threshold is (derived from (51) in [8])

$$\phi_c = \{(5/P)[2\exp(u/kT)+3]\}^{1/2}/6[\exp(u/kT)-1] \tag{25}$$

which is a decreasing function of the repulsive interparticle potential ($u$) shown in figure 2, where $P = 0.68$ is a theoretical value in the calculation for the packing of stable hard spheres [8]. At moderate repulsive potentials, (25) scales simply as $\phi_c \sim (u/kT)^{-1.34}$ for $u/kT \leqslant 2$. Figure 2 reveals that a decrease in temperature or an increase in repulsion, which arises with either charged particles at low ionic strengths or adsorbed polymer layers, can result in lower $\phi_c$ [4, 23]. We shall not pursue the details of this discussion as it lies somewhat outside the focus of this paper.

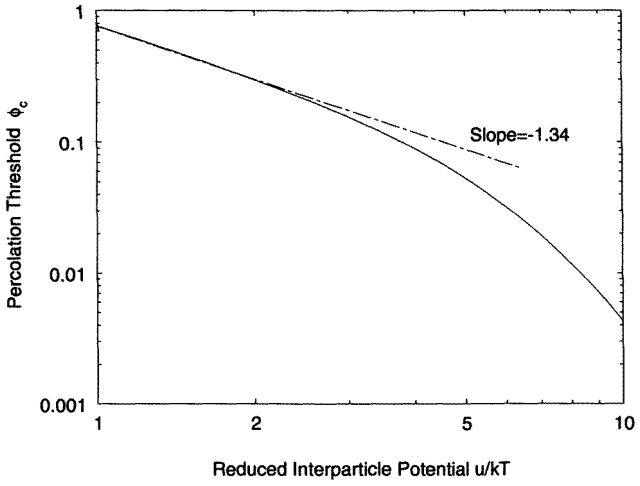


**Figure 2.** The relationship between the critical volume fraction and the repulsive interparticle potential in stable colloidal dispersions.

We have theoretically determined $u/kT = 1.25$ for a neutrally stable hard-sphere system [8], which gives $\phi_c = 0.5733$. This value is very close to the measured critical volume fraction [24]. $\eta_r(0,\phi)$ diverges as $\phi \to \phi_c$. (22), (24), and (25), and experimental data [1, 5] for polystyrene lattices in water and for silica spheres in cyclohexane at the limits of low and high shear rates, are compared in figure 3. Here we have re-emphasized the important difference between the low and high curves which get bigger as $\phi$ increases. Below volume fractions of 0.3, no shear thinning can be detected [1, 4]. Figures 4–6 are the result of numerical calculations from (20)–(22) and (24). In figure 4, the relative shear viscosities at different volume fractions are plotted against the dimensionless shear rate in the vicinity of the percolation threshold. By using (11), the relationships between the shear stress and shear rate are obtained as a function of $\phi$ in figure 5. From figures 4 and 5, the

dependence of the relative shear viscosity on the reduced shear stress is shown in figure 6, where a dramatic effect of shear thinning in the vicinity of the percolation transition is seen. This explains what has been reported recently in the literature [2]. The reduced shear stress is $\sigma_r = a^3\langle\sigma_{yz}\rangle/kT$. The transition in figure 6 also occurs when $\sigma_r$ is close to unity. Therefore, the macroscopic shear stress is at least comparable to the instantaneous shear modulus (see (30)), and a nonlinear flow behaviour is expected for the system. It may be worthwhile to point out that no adjusting parameter has been introduced in the present theory, besides the pre-determined repulsive interparticle potential already mentioned.

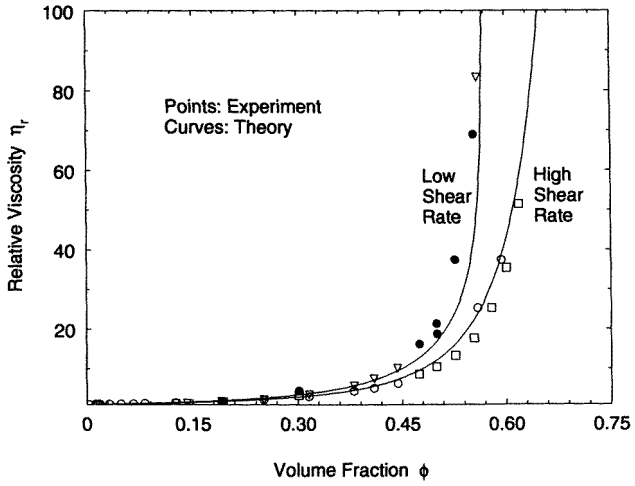


**Figure 3.** A comparison of the calculated and measured [1, 5] limits of shear viscosity as a function of volume fraction for polystyrene lattices in water and silica spheres in cyclohexane.

In the case of oscillatory shear flow, the dynamic shear viscosity $\eta(\omega, \phi)$ is linked to the memory function $M$ by

$$\frac{\eta(\omega,\phi) - \eta_\infty(\phi)}{\eta_0(\phi) - \eta_\infty(\phi)} = M[\omega\tau(\phi)] = \int_0^\infty M(s)\exp[-\mathrm{i}s\omega\tau(\phi)]\,\mathrm{d}s \tag{26}$$

where $\omega$ is the angular frequency, $\tau$ is the macroscopic relaxation time, and the limits of viscosity share the expressions given by (22) and (24). We have derived [8]

$$M(s) = -\mathrm{d}K(s)/\mathrm{d}s = (1/2s^{1/2})\exp(-s^{1/2}) \tag{27}$$

where $K$ is the relaxation function. (26) and (27) correlate well with experimental data [3]. There are significant differences between $M$ in (26) and $Q$ in (21). $M$ is a function of $\omega\tau$ only and is independent of $\eta_0$ and $\eta_\infty$. In contrast, $Q$ is a nonlinear function of $\eta$ which depends on the limiting viscosities. By using (27), the asymptotic expression of (26) is

$$M[\omega\tau(\phi)] = 0.627(1 - \mathrm{i})[\omega\tau(\phi)]^{-1/2} \qquad \text{as } \omega \to \infty. \tag{28}$$

This $-1/2$ power law decay in frequency is derived for the dynamic viscosity in oscillatory shear flow; however, it is not applicable to describe the shear rate dependence of the nonlinear viscosity in steady state shear flow.

Both (27) and (28) are derived from a distribution function which is governed by a generalized diffusion equation having the same form as (8) except with $\boldsymbol{v} = \mathbf{0}$. The shear-induced microstructure has a Gaussian distribution (see equations (19) and (20) in [8]) for

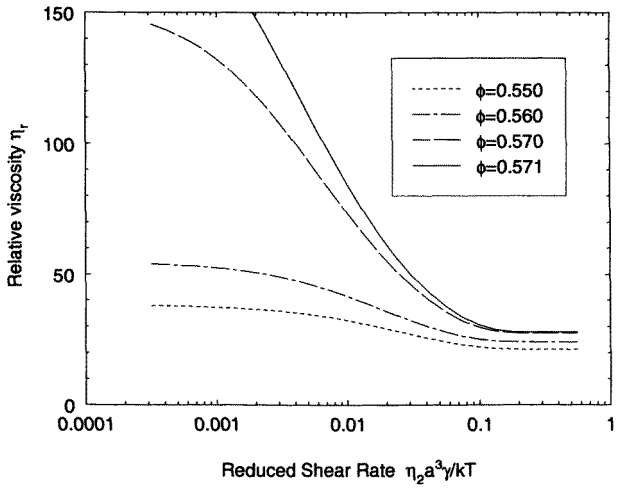


**Figure 4.** The nonlinear viscosity in steady state shear flow versus the nondimensional shear rate in the vicinity of the percolation transition.

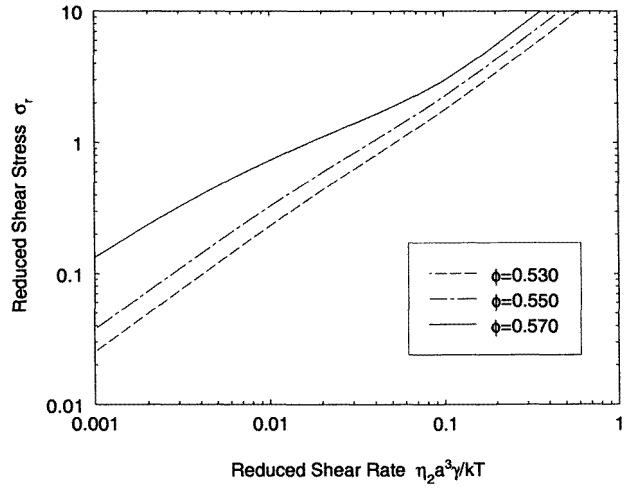


**Figure 5.** Nonlinear shear stress and shear rate relationships at different volume fractions of highly concentrated dispersions.

linear oscillatory shear flow, but has a non-Gaussian distribution for nonlinear steady state shear flow where a significantly larger displacement in the flow field occurs.

The relaxation time and the zero-shear viscosity can be related by

$$\eta_0(\phi) = G_0 \int_0^\infty K[t/\tau(\phi)]\,\mathrm{d}t = 2G_0\tau(\phi) \tag{29}$$

where the unrelaxed shear modulus $G_0$ is assumed to be much larger than the relaxed modulus, and (27) has again been used in (29). The relaxation time is also proportional

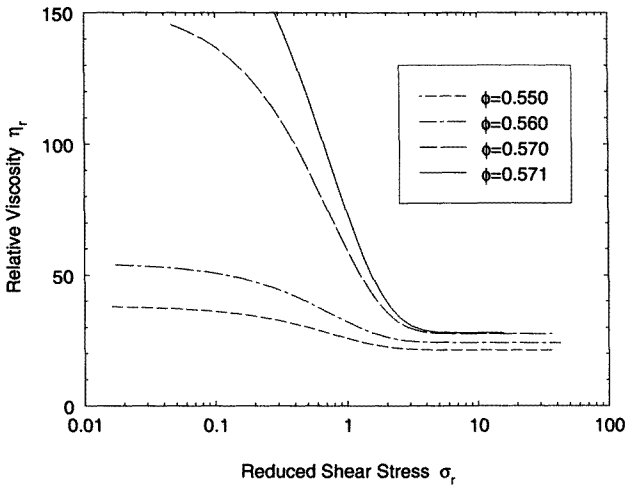


**Figure 6.** The nonlinear viscosity in steady state shear flow versus the reduced shear stress in the vicinity of the percolation transition.

to the characteristic time of Brownian motion ($a^2/D_0$), where $D_0 = kT/\zeta_0$ is the Stokes–Einstein diffusion coefficient. Since $D_0$ and $G_0$ are independent of $\phi$, we have

$$\tau(\phi) = \eta_0(\phi)/2G_0 \sim (a^2/D_0)\eta_r(0,\phi) \qquad G_0 \sim kT/a^3 \tag{30}$$

where $\eta_r(0,\phi)$ is given by (24). A comparison between the above equation and the experimental data for silica in cyclohexane is shown in figure 7. We see a sudden increase in $\tau(\phi)$ as $\phi$ approaches $\phi_c$. Thus, there is a time–composition superposition for $M$ in the $M$ versus $\omega\tau$ plot (see figure 9 in [3] and figure 1 in [8]), but not for $Q$ in the $Q$ versus $\eta_2 a^3\gamma/kT$ plot, where the nonequilibrium microstructure is affected nonlinearly by shear flow.

## 6. Conclusions

Analytical expressions, (20) and (21), for the effective shear viscosity of concentrated dispersions in steady state shear flow have been derived as a function of the volume fraction, particle size, interparticle potential, and shear rate (or shear stress). Besides the pre-determined repulsive interparticle potential, there is no adjusting parameter in (20)–(22), (24) or (25). The predicted shear-rate-dependent viscosity (figure 1) and relaxation time (figure 7) of neutrally stable dispersions are in good agreement with experimental data.

The microscopically based constitutive equation shows dramatic shear thinning in the plots of the nonlinear viscosity versus shear stress as $\phi$ approaches a critical value $\phi_c$, which depends on the repulsive interparticle potential. Our theory explains an important non-Newtonian phenomenon in colloidal dispersions—the shear rate has negligible effect on the nonlinear effective viscosities at low $\phi$, but has a dominant effect at high $\phi$. There is a dramatic shear thinning effect in the vicinity of the percolation transition.

The shear-induced microstructure has a Gaussian distribution for linear oscillatory shear flow, but has a non-Gaussian distribution for nonlinear steady state shear flow. This results in a fundamental difference between $M$ and $Q$. The memory function $M$ in oscillatory shear

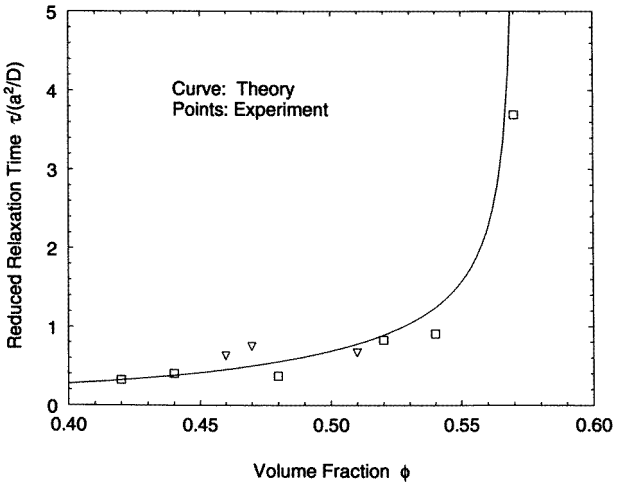


**Figure 7.** Calculated and measured relaxation time compared as a function of volume fraction for silica spheres in cyclohexane [3].

flow is a function of $\omega\tau$ only. The memory function $Q$ in steady state shear flow depends not only on the shear rate, particle size, and volume fraction, but also on the effective shear viscosity, which has to be solved simultaneously with (20)–(22), (24), and (25). Therefore, there is a time–composition superposition for $M$ (see figure 9 in [3] and figure 1 in [8]), but not for $Q$. This leads us to a familiar classification of viscoelastic behaviour: the linear dynamic viscosity in oscillatory shear flow is rheologically simple, but the nonlinear viscosity in steady state shear flow is rheologically complex.

## References

[1] Krieger I M 1972 *Adv. Colloid Interface Sci.* **3** 111
[2] Buscall R 1992 *Theoretical and Applied Rheology* vol 2, ed P Moldenaers and R Keunings (Amsterdam: Elsevier) p 591
[3] Van der Werff J C, de Kruif C G, Blom C and Mellema J 1989 *Phys. Rev.* A **39** 795
[4] Russel W B, Saville D A and Schowalter W R 1989 *Colloidal Dispersions* (Cambridge: Cambridge University Press) ch 14
[5] de Kruif C G, van Iersel E M F, Vrij A and Russel W B 1985 *J. Chem. Phys.* **83** 4717
[6] Cichocki B and Felderhof B U 1992 *Phys. Rev.* A **46** 7723
[7] Brady J F 1993 *J. Chem. Phys.* **99** 567
[8] Chow T S 1994 *Phys. Rev.* E **50** 1274
[9] Bird R B, Armstrong R C and Hassager O 1987 *Dynamics of Polymeric Liquids* vol 2, 2nd edn, (New York: Wiley)
[10] Doi M and Edwards S F 1986 *The Theory of Polymer Dynamics* (Oxford: Clarendon)
[11] Dyre J C 1993 *Phys. Rev.* E **48** 400
[12] Kirkwood J G 1967 *Macromolecules* (New York: Gordon and Breach)
[13] Batchelor G B 1977 *J. Fluid Mech.* **83** 97
[14] Anderson P W 1963 *Concepts in Solids* (Reading, MA: Benjamin)
[15] Wood D M and Ashroft N W 1977 *Phil. Mag.* **35** 269
[16] Chow T S 1980 *J. Mater. Sci.* **15** 1873
[17] Chow T S 1993 *Phys. Rev.* E **48** 1977
[18] Chow T S 1973 *Phys. Fluids* **16** 31

[19] McCrum N G, Read B E and Williams G 1967 *Anelastic and Dielectric Effects in Polymeric Solids* (New York: Wiley)
[20] Mooney M 1951 *J. Colloid Sci.* **6** 126
[21] Feynman R P 1972 *Statistical Mechanics* (Reading, MA: Benjamin)
[22] Kirkwood J G, Buff P F and Green M S 1949 *J. Chem. Phys.* **17** 988
[23] Woutersen A T J M and de Kruif C G 1991 *J. Chem. Phys.* **94** 5739
[24] D'Haene P, Fuller G G and Mewis J 1992 *Theoretical and Applied Rheology* vol 2, ed P Moldenaers and R Keunings (Amsterdam: Elsevier) p 595